Analysis of battery lifetime extension in a SMES-battery hybrid energy storage system using a novel battery lifetime model

Jianwei Li, Anthony M. Gee, Min Zhang, Weijia Yuan*
Department of Electronic and Electrical Engineering, University of Bath, United Kingdom

Abstract— In off-grid wind energy systems batteries often undergo frequent charge discharge cycles, which reduce battery service life. In addition, due to motor start and other high 'inrush current' loads batteries can also undergo high rates of discharge which also degrade battery life. In this paper, a superconducting magnetic energy storage and battery hybrid energy storage system is proposed which is beneficial in reducing battery short term power cycling and high discharge currents. To demonstrate system performance, a representative off-grid wind power system model is described in detail which incorporates turbulent wind variations, load variations and energy storage systems. To estimate battery lifetime improvement, a novel battery lifetime model is described which quantifies the impact of both the number of charge/discharge cycles and also the effect rate of discharge. The model is validated using previously reported data. This work advances previous studies by describing the estimated improvement in terms of battery life in a wind energy conversion application by use of superconducting energy storage and by presenting a novel method for doing so. In addition, the proposed battery lifetime model can be potentially used in other applications.
Key Words— superconducting magnetic energy storage (SMES), battery, off-grid wind power system, battery lifetime model, discharge rate

1. Introduction

The variable nature of wind and fluctuating load profiles make the operation of off-grid wind energy power systems challenging as the load requirement is unlikely to match the available power from the wind resource. To ensure security of supply by preventing the load from being unsupported, some form of energy storage system (ESS) is typically integrated into the system to store power from times when there is a surplus and to release it during a deficit of available power [1].Typically in remote off-grid power systems, this energy storage system has been a secondary or rechargeable battery [2-4].One of the main disadvantages of this form energy storage in renewable energy systems has been shown to be a limited cycle-life [2, 5] and sensitivity to high peak discharge rates [6]. For a wind turbine based off grid wind energy conversion system, an ideal ESS would be able to provide both high power and energy capacity to be able to support turbulent wind power gusts and high peak discharge currents and also provide a high cycle life to ensure reliable operation and reduced system costs. Compared with other energy storage technology the principle advantages of SMES are: high power density, high cycle-life, high discharging efficiency and high peak current handling capabilities [1, 7-9]. For this reason, the study presented below proposes the hybridization of superconducting magnetic energy storage and battery energy storage to create a hybrid energy storage system capable of extending battery service life.

*Corresponding author. Tel.:+44 1225386049/7726759745;fax:+441225386305.
Email address: w.yuan@bath.ac.uk (Weijia Yuan); jl977@bath.ac.uk (Jianwei Li).

In terms of storage duration, energy storage systems can typically be categorized into short-term

storage systems including flywheels[10], super-capacitors [11] and SMES[12] and long-term systems such as secondary (rechargeable) batteries. Typically long-term storage has a higher energy density but lower power density and cycle life, while short-term energy storage system is characterized by high power capacity[13]. The active combination of two or more energy storage technologies can yield various advantages. In [14, 15] the authors have hybridized short-term and long-term ESSs into electric vehicles achieving higher power, greater energy delivery, longer all-electric range and improving system efficiency. Wei et al. [16] and Sarrias-Mena [17] have introduced a battery/super-capacitor HESS into wind applications to improve overall system efficiency and reduce the system cost by increasing battery life. A SMES/battery HESS is designed in [18] which was successfully used in railway substations to compensate fluctuating loads. Zhou et al. [19] have shown that the combination of short-term ESS and long-term battery energy storage guaranteed a better penetration of renewable energy into the power system. Gee and Dunn in [20] have described a method in which the battery life extension can be improved in an off-grid wind power system using super-capacitors. Also, battery lifetime was successfully predicted in other studies [21-24] using a similar method. However, these studies [20-24] have calculated battery lifetime consumption by only quantifying the impact of charge/discharge cycles in different depth of discharge (DOD) but neglecting the effects of discharging current. Previous work [14-20, 25] has shown that the extension of battery lifetime is one of the biggest advantages of hybridizing battery energy storage with a short term energy storage system. Therefore, the study presented herein, describes a method in which battery life can be extended by use of a superconducting energy storage system. The effect of hybridization is shown to not only in reduce battery charge/discharge cycling but also to reduce peak discharge current. For this reason, this study contributes to and extends previous work by describing a novel means by which the effect of discharge current magnitude can be quantified in terms of battery service life reduction. As the main contribution of this study, the novel battery lifetime model is verified by case studies and results indicate that the improved battery lifetime model gives a more accurate prediction.

2. System design

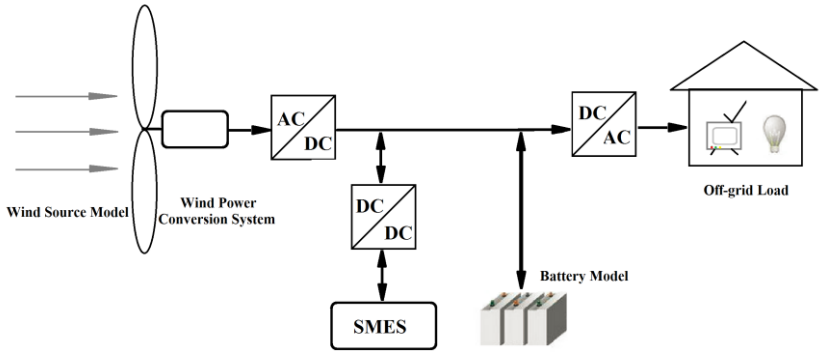

Fig. 1. Remote wind power system with HESS

A representative dynamic off-grid power system including wind turbine, battery, SMES, power

converters and load has been developed in Matlab/Simulink and used to demonstrate the operation of the HESS (Fig. 1). A model of wind source based on real wind data is established. In addition, the high-frequency turbulence has been add to the wind source model so that to effectively simulate the performance of the variations of wind speed [26]. The wind turbine is modeled based on the commercially available generator model (Table A in Appendix) using the method described in [27]. The power output from the wind turbine is fed to the battery, SMES and load. In this study, a realistic domestic house hold load profile [20] is used in the off-grid system. The SMES is connected to the DC bus via a DC/DC chopper and it is modeled following the introduction of [12].SimPower-Systems toolbox in Simulink has offered a battery block to implements a generic dynamic model parameterized to represent rechargeable batteries. In this study, technical characteristics of Li-ion batteries in the HESS are assessed using this model. To enables the long-term simulation of the whole system and reduces computational effort the power converters are modeled as equivalent efficiency factors following the method given in [20]. In addition, system control algorithm and sizing study is introduced in this section.

2.1 Control algorithm

In order to reduce the usage of fossil fuels as much as possible, the system is designed such that ESS and wind turbine is sized to match the load at all time. A coordinated control strategy for hybrid energy storage in a remote area wind power system is proposed in this study. The control coordination algorithm takes the different conditions of wind turbine, the various loads, the battery and the SMES into account to prove the benefits of the proposed HESS.

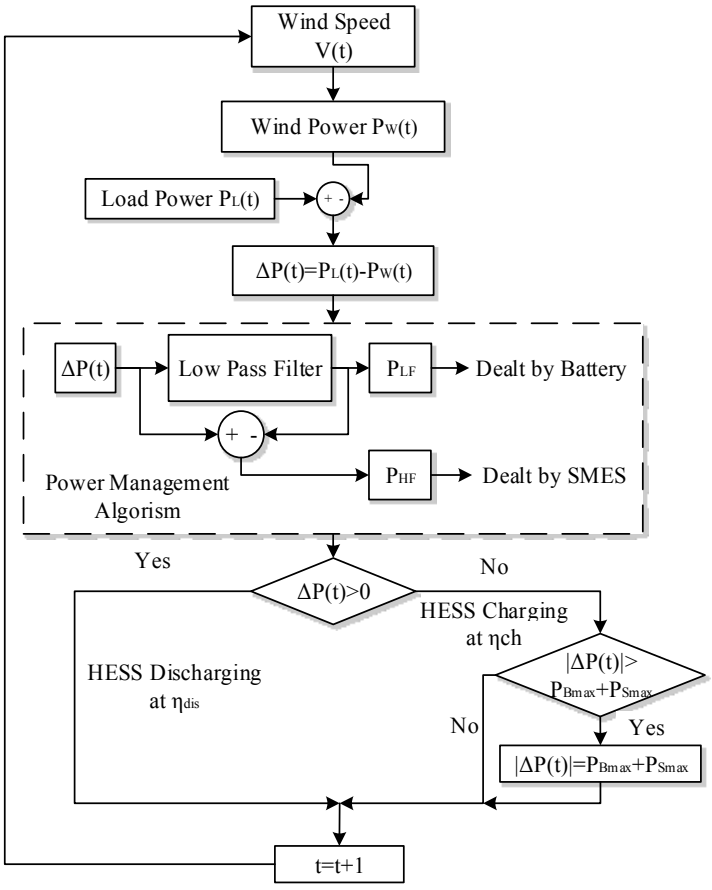

Fig. 2. Control coordination of a SMES-battery HESS in an off-grid wind application

The power control algorithm is shown in Fig. 2:

- During the windy period when the generated power from the wind turbine $P_w(t)$ is greater than the load demand $P_L(t)(\Delta P(t) = P_L(t) - P_w(t), \Delta P(t) < 0)$, the HESS will be charged by the excess power ($\Delta P(t)$). According to the Power Management Algorithm (PMA) as shown in Fig. 2, the high frequency component (P_{HF}) of the excess power will charge the SMES; while, the battery is charged by the low frequency component (P_{LF}) of $\Delta P(t)$. Assuming the rated power of the SMES is P_{Smax} and that for battery is P_{Bmax}. If the excess power is greater than the summation of P_{Smax} and P_{Bmax}, the over-charging protection will come into effect and make $\left|\Delta P(t)\right| = P_{Smax} + P_{Bmax}$.
- During the generation-deficiency condition where the wind power cannot meet the load demand $(\Delta P(t) = P_L(t) - P_w(t), \Delta P(t) > 0)$, the HESS is designed to be discharged and support the required power deficit $\Delta P(t)$. According to the PMA, the battery will deal with the long-term component and SMES will supply the short-term component. The HESS is sized (see Section 5) to be flexible enough to deal with all the situations for a remote area power system. Hence, the HESS can always supply the power deficit.

To sum up, this coordinated control algorithm can guarantee an active combination of two kinds of different ESSs and achieves the following objectives:

- Successfully combined long-term and short-term storage systems achieving a stable and fast HESS.
- Improve the life-cycle of battery by reducing the charge/discharge frequency and lowering high rate of battery discharge current.

The performance of superconducting energy storage system in a battery ESS has already been investigated in [18, 28], but these studies only focused on SMES. Also, the simulation periods (30 minutes in [18], 20 seconds in) were not long enough to study the performance of battery and interaction between battery and SMES. To study the improvement of battery lifetime in the HESS, two weeks are selected as the time duration in this study.

2.2 System sizing study

Based on the described system in Section 1, for a given load and a wind turbine in a remote area, three elements battery and SMES should be sized to balance the power/energy and to mitigate fluctuations. As SMES is a type of short-term energy storage technology, it cannot store much energy [7]. Therefore, it is reasonable to divide the sizing study into two steps. The first step is to do integrated sizing study of battery to guarantee that the load is always met. Secondly, the SMES is sized to make sure the undesired high frequency component is absorbed.

The concept of "Loss of Power Supply Probability" (LPSP) which describes the probability that the load cannot be met is chosen as a reliable measurement for battery sizing study. The LPSP is the ratio of total energy deficit over the total load demand and the LPSP approach has already been used in many studies [29-31]. For a given load and a wind turbine (Table A in Appendix), the battery is sized to be 244Ah using LPSP method.

As illustrated in the control algorithm, SMES is designed to support the high frequency component

(P_{HF}) of fluctuated power ΔP. SMES has a high power density and can offer an immediate power supply but unable to store large amount of energy. Therefore, it is reasonable to size the SMES based on the capability of storing energy rather than the power to guarantee the reliability of the HESS. In this paper, two constraints are taken into account to determine the size of SMES and the sizing study is based on the simulation result of the PMA described in Section 3.

Firstly, focusing on the long-term duration, the rated energy capacity of SMES E_{SMES} should be greater than the integration of power over simulation period as shown in Eq. (4) where the total simulation time is T_s. When $P_{HF} > 0$, the SMES will be discharged and deliver energy to the system; when $P_{HF} < 0$, the SMES will be charged and absorb energy.

$$E_{SMES} \geq \int_0^{T_s} P_{HF} dt \quad (4)$$

Secondly, considering the single cycle which has the biggest P_{HF}, the rated energy capacity of SMES (E_{SMES}) should be greater than the energy that stored or released by the biggest cycle. Hence Eq. (5) can be used to describe another sizing constraint for SMES.

$$E_{SMES} \geq \int_0^{T_{max}} |P_{HF}|_{max} dt \quad (5)$$

Where $|P_{HF}|_{max}$ is the peak value of P_{HF} and T_{max} is the biggest cycle period during the simulation time. The energy stored in a SMES coils given in (6) is determined by the current I flowing the coil and the inductance L of the coil.

$$E_{SMES} = LI^2/2 \quad (6)$$

Due to the good performance[32], the second-generation high-temperature superconductor is selected to design the SMES. The configuration which is determined the coil inductance L has great impact on the maximal stored energy. Hence, optimal configuration algorithm is done according to [33]. Based on the sizing study of SMES, a 2kJ double pancake SMES coil is designed as shown in Fig. 6 and the parameters are shown in Table A.2 with low-pass filter cut-off frequency of 0.002 Hz.

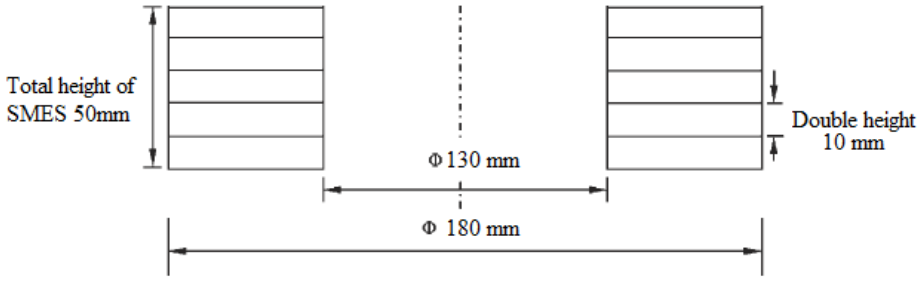

Fig. 6. Design of double pancake coil.

Simulation results in Section 7 showed that the 2kJ SMES integrated with 244 Ah battery could meet the requirement of mitigating the fluctuations of wind power and balancing the power supply and load demand.

3. Battery lifetime modeling

The extension of battery-life is one of the key metrics for assessing the benefits of a SMES-battery hybrid energy storage system [14-20]. Therefore, it is necessary to incorporate a battery-life prediction model in this research. The life of rechargeable battery is defined as the period that the battery remains serviceable before the predefined minimum capacity (normally 80%) reached. Various kinds of battery-life models are available. However, the capacity fading mechanism is so complicated that it is currently can hardly to create a practical model which considers the extreme non-linearity of many underlying aging processes [34]. Therefore, some simplified battery-life estimation models are developed such as rain-flow cycle counting model [35]. Experiments have been done by Bindner in [36] aiming to compare several battery life models and the results showed that the cycle counting algorithms generate a relatively more accurate prediction.

This method of cycles counting has already been successfully employed in battery lifetime estimation applications [24, 35, 36]. In addition, the battery life prediction method is successfully applied in a commercial program known as HYBIRD2[21] .However the previous work simply counted the number of cycles for each level of depth of discharge (DOD, normally refers to the extent to which batteries are discharged). It means that the conventional battery life model only regarded the range of DOD of each cycle as the factor related to battery lifetime, but neglected other factors such as discharging rate. James F. Manwell proposed an improved model in[21] by adding the effect of the mean value of each charge/discharge cycles, but this improved model did not consider the discharging rate which has great impact on the battery life.

Discharging rate is referred as discharging current and often expressed as a Crate by normalized means. Crate is normally regarded as the rate at which a battery is discharged relative to its maximum capacity[37]. Many research works [22, 38-40] have shown higher discharging rates would shorten the battery life dramatically. For example, experiments have been done in [40] to study the capacity fade of Sony 18650 batteries under different Crates. The results showed that battery lost 9.5% of its capacity after the full 300 cycles at 1 Crate, but the number almost doubled for 3 Crate (16.9%). Therefore, the impact of Crate on battery life is so great that should not be neglected.

This paper proposes a novel battery life model which has quantified both the effect battery discharging rate and depth of discharge and gives a more precise prediction for battery lifetime. Error analysis has been done by means of two case studies which comparing the computed results from the novel model with experimental results from two different experiments.

3.1Rain-flow cycle-counting algorithm

A rain-flow cycle-counting algorithm normally used for analyzing the fatigue data and was firstly used metal fatigue estimation. In this research, this method is used to extract the irregular charging and discharging cycles that the battery experienced during the simulation period.

Simulation result gives an array of DOD which is used as the major inputs in this algorithm. Based on [41], the process for battery cycle-counting can be illustrated in three steps.

- Firstly the variation data of DOD of battery is pre-processed by searching for adjacent data points with reverse polarity so that the local maxima and minima can be found and stored in a matrix. In addition, exact time of occurrence of turning points is stored in the same matrix.
- Secondly, combine these sub-cycles to get full-cycles together with the summing up of the amplitudes and time durations.
- Thirdly, extract the number of cycles in varying amplitude and time duration and store them for later use.

As a result, the complex data can be resolved into a set of equivalent sub-half-cycles and rearranged composing series full-cycles of different amplitude and start-end time. Hence each cycle is stamped by two elements that the depth of discharge and discharging rate (Crate). For a given depth of discharge, the discharging rate can be calculated by Eq. (7)

$$Crate = \frac{\mathrm{A}}{\mathrm{T}/3600} \quad (7)$$

Where A is the amplitude of DOD, T is the cycle period and 3600 means 3600 seconds in an hour.

3.2 The novel battery life-cycle modeling

For a rechargeable battery, the active substance transformed with each cycle is proportional to the range of discharging [42]. Therefore the deeper the battery is discharged the more life-time will be consumed. Battery manufacturers usually provide the experiment datasheet to describe the relationship between battery cycle life and DOD. Fig. 7 gives a typical Cycles to Failure (CTF) vs. DOD curve obtained by curve fitting using experiment data the for lithium battery from manufacture at a given discharging rate (1 Crate).

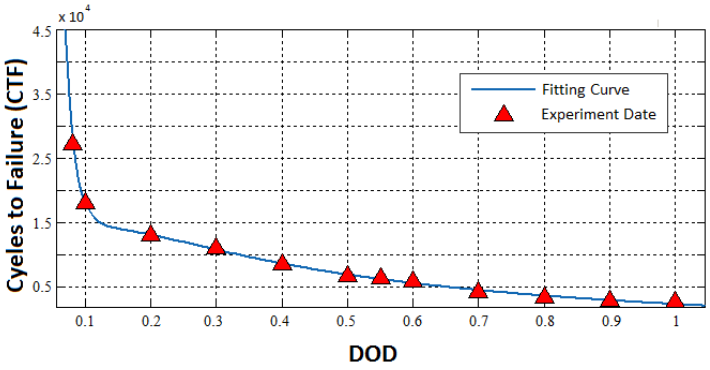

Fig. 7. Cycles to failure vs. DOD curve

Battery CTF is defined as the number of cycles that the battery can be charged and discharged before the end of life condition is reached [20]. For example, as it can be observed in Fig. 7, the battery would undergo over 5000 cycles at 60% DOD before it reached the end of life. Therefore, Battery cycle-counting models are based on the assumption that the charge cycle amplitude determines the fraction of lifetime that is consumed based on CTF vs. DOD curve. A logarithmic polynomial function F_{CD} is used to describe the relationship between the CTF and the DOD $F_{CD} = f(CTF, DOD)$:

$$CTF = f_{CD}(DOD) = a_0 + a_1 DOD^{-1} + a_2 DOD^{-2} + a_3 DOD^{-3} \quad (0 < DOD \le 1) \ (8)$$

Where $a_0 - a_3$ are the curve fitting coefficients and respectively, the values for them are -4790, 7427, -1077, 55.4.

Previous work [40, 43, 44] has shown the functional relationship of the capacity retention and discharging current. Based on the experiments that described in [43], this paper defines the function F_{CC} to show that the capacity retention of a Li-ion battery will decrease with the increase of the discharging current $F_{CC} = f(CRate, Cpacity)$:

$$Capacity = f_{CC}(Crate) = b_0 + b_1 \times e^{-\left(\frac{Crate - b_2}{b_3}\right)^2} \quad (0 < Crate) \quad (9)$$

Where $b_0 - b_3$ are the curve fitting coefficients and respectively, the values for them are 0.8800, 0.0929, -0.0639, -1.3770.

In general, the capacity retention of a Li-ion battery is proportional to the battery life-cycles [45]. Function F_{CTFC} is defined in this study to describe the how the CTF changes with the capacity of Li-ion battery, $F_{CTFC} = f(CTF, Cpacity)$:

$$Capacity = f_{CTFC}(CTF) = c_0 + c_1 \times CTF \quad (10)$$

Where c_0, c_1 are the curve fitting coefficients and they are -0.00177 and 0.96.

As a result, for a charge/discharge cycle with the given range of DOD and Crate, the objective function can be obtained by combining the Eq. (8)-(10), $F_{CDC} = f(CTF_C, DOD, CRate)$:

$$CTF_C = f_{ND}(DOD) \times f^{-1}{}_{CTFC}(f_{CC}(Crate)) \quad (11)$$

CTF_C is the corrected CTF number. Define the degradation factor as η, as the degradation of battery by a charge/discharge cycle at certain range of DOD and Crate, then:

$$\eta = 1/CTF_C \quad (12)$$

The algorithm of the novel battery lifetime model is shown in Fig. 8. As shown in Fig. 8, the rain-flow cycle-counting algorithm processed the data of DOD of battery obtaining the different cycles varying in different ranges of DODs and Crates in a matrix. Take the cycle i as an example: Substitute DOD_i into F_{CD} obtaining the original number of cycles N_i. Similarly, F_{CC} generates the capacity fading factor $\varepsilon_I(\varepsilon_i = f_{CC}(Crate_i))$ t the given $Crate_i$. This factor is a capacity related factor hence F_{CTFC} is needed to transfer it into a cycle number related factor $\varepsilon_i'(\varepsilon_i' = f^{-1}{}_{CTFC}(f_{CC}(Crate_i)))$. The original number N_i multiplied by factor ε_i' resulting in the corrected number of cycles N_{ic} at $Crate_i$ and DOD_i. Therefore the consumed fraction of battery life after the charging/discharging cycle i is $\eta_i = 1/N_{ic}$. The total number of different cycles is n, hence the total degradation D is:

$$D=\sum_{i=1}^{i=n}\eta_i \quad (13)$$

Assuming the simulation duration is T, hence the battery lifetime can be estimated:

$$L_B = T/D \quad (14)$$

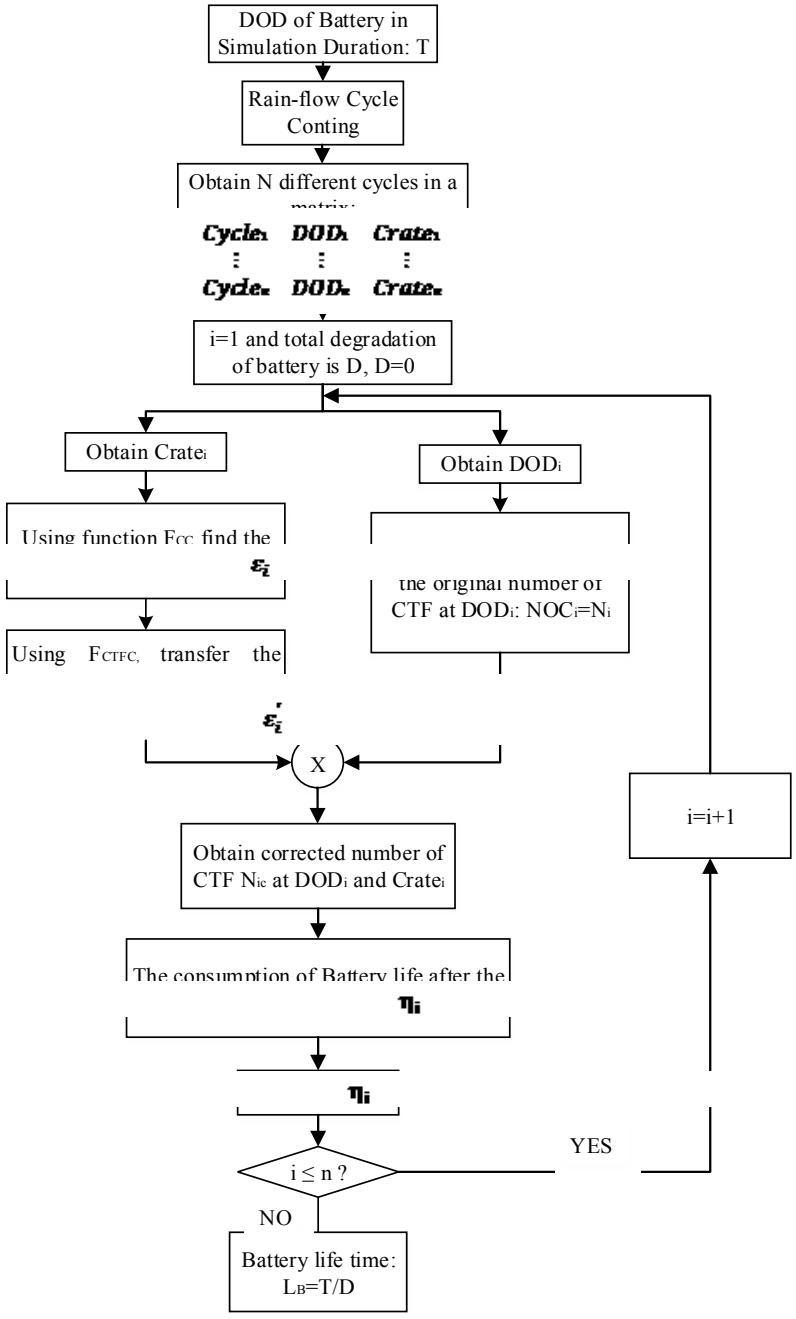

Fig. 8. Algorithm of the novel battery lifetime model

The error analysis of the proposed algorithm is fulfilled by the following case study. It should be noted that the novel battery model is based on the room temperature.

3.3 Case study

The novel battery lifetime model is valued for taking the discharging rate into account. Hence two case studies that based on different experiments have been done to prove the validity of the new model.

2.31 Case study 1

The novel battery lifetime model is valued for taking the discharging rate into account. Hence a case study was done to prove the validity of introduce of Crate. Li-ion battery accelerated aging tests by [22] showed results describing that the normalized capacity retention declined as a function of at different rates and fixed DOD of 0.3. The capacity retention limit is defined as 80%, which means the end of battery life. Based on [22], the experimental battery lifetime at different Crate can be obtained as shown in Table 2. For example, the experimental battery lifetime as described in Table 2 is 3300 hours by uninterrupted discharging battery in 1.5 Crate.

Table 2 Experimental Battery lifetime at different Crate[22]

Crate	0.6	1.2	1.5	1.8
Lifetime(h)	8800	4300	3300	2800

Based on the algorithm illustrated in Fig. 8, if the DOD is set as 0.3 and Crate as 1.5 the following data can be obtained: (Based on Eq. (7), Crate=1.5 means that battery is discharged 30% of its capacity in 0.2 hour hence the whole cycle time is 0.4 hour)

Table 3 Calculated data based on the novel model at a given Crate 1.5

Original cycle number	Capacity fading factor	Cycle related factor	Corrected cycle number	Consumed fraction η	Cycle time(h)	Battery life (h)
10052	0.906	0.86	8600	1.162e-4	0.4	3440

The error between the calculation and experiments is 4.2% which is acceptable. However, if the impact of discharging rate is not considered, the lifetime is 4021 h (cycle time (0.4 h) multiplied by original cycle number (10052)) and the error is 21.8%. Appling the same process to the other three situations, Table 4 and Fig. 9 could be made as followed:

Table 4 Comparison of experimental results with the results based on novel battery lifetime model and results from the previous model

Crate	Experimental battery lifetime(h)	Novel model based battery lifetime(h) and error	Cycle time(h)	Previous model based battery lifetime(h) and error
0.6	8800	9185, 4.38%	1.00	10052, 14.2%
1.2	4300	4430, 3.02%	0.50	5026, 16.8%
1.5	3300	3440 , 4.2%	0.40	4021, 21.8%

1.8	2800	2930, 4.6%	0.34	3418, 22.1%

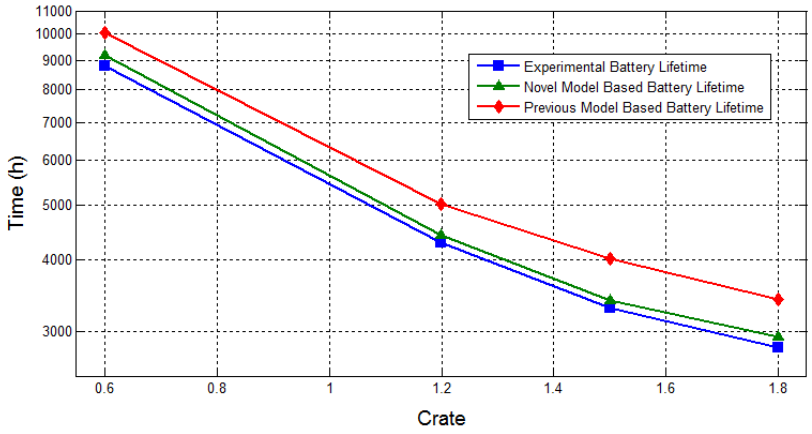

Fig. 9. Comparison of battery lifetimes base on experiments (blue), the novel model (green) and the previous model (red).

Obviously, this new algorithm which has taken the discharging rate into account, is valued for its smaller error and gives a more precise perdition of battery lifetime hence a batter battery life-cycle model.

2.32 Case study 2

Case study 2 is based on the test described in [40] about capacity fade study of Li-ion batteries at different discharge rates. According to [40], capacity fade of Li-ion batteries cycled up to 300 times using 1C, 2C and 3C discharging rates is quantitatively measured on the Arbin Battery Test System and the electrochemical characterization of the batteries have been studied using the Solartron SI 1255 HF Frequency Response Analyzer. The results show that the capacity losses were estimated as 9.5% at 1C and 13.2% at 2C after 300 fully discharged cycles whereas the number reach to 16.9% at 3C.

In this case study, the battery life or capacity degradation is calculated by both the previous and the novel algorithm following the condition (fully discharged batteries 300 times at 1C, 2C and 3C) described in [40]. Based on the previous method, the capacity degradation remains unchanged as 11.7% at three different Crate. However, using the novel algorithm the estimated capacity degradation is 11.9%, 12.8% and 14.9% at 1C, 2C and 3C, respectively. Fig. 10 compere the estimated data of the two models with the experimental data.

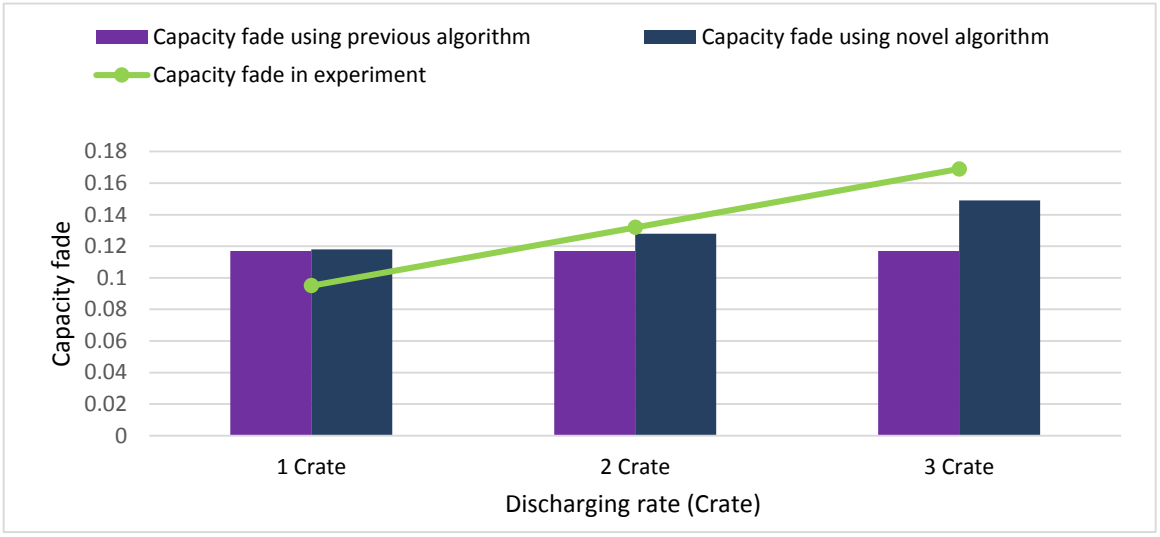

Fig. 10 Comparison the estimated capacity fade in the precious and the novel models with the experimental result

As shown in Fig. 10, the capacity degradation will increase with the growth of Crate in experiment. The prediction given by the novel method shows a similar tendency with the experimental data. However, the capacity fade at all the three Crate is estimated as a same value using the previous method. Therefore, the novel algorithm gives a better estimation of capacity degradation hence an improved battery lifetime perdition model. In addition, as can been seen in Fig. 10, there are still some errors between the experimental data and the prediction data using the novel model. This because of the inherent errors in the proposed test and some other factors that have not been considered in this model such as operation temperatures.

4. Simulation results and discussions

The whole system with control strategies is built in Matlab/Simulink. In order to study the battery life extension in a HESS, two weeks is selected as the simulation period.

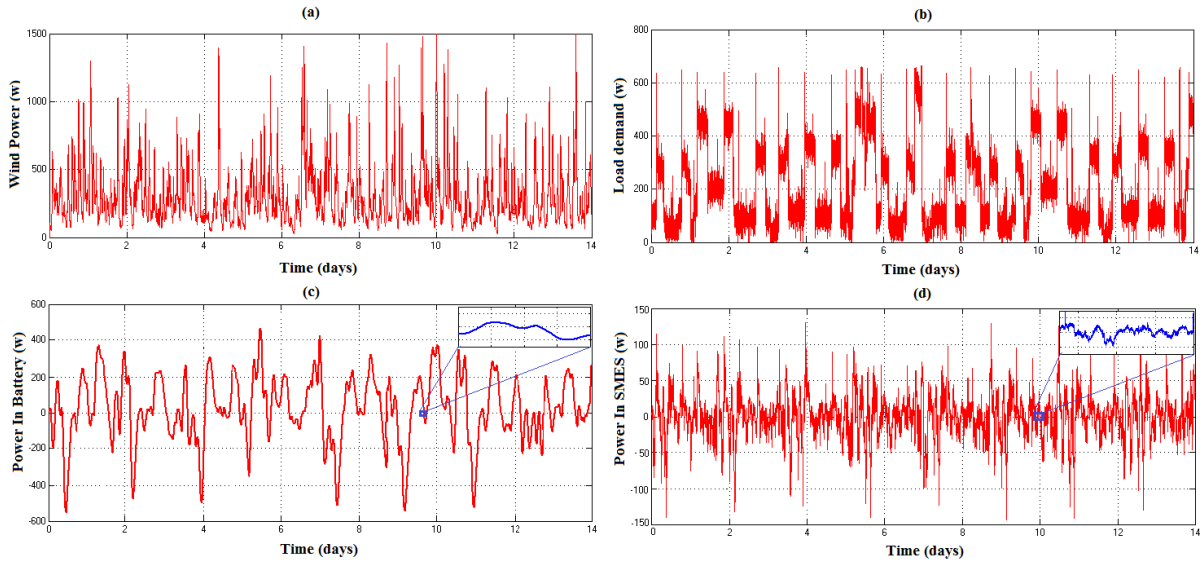

Fig. 10. Simulation results for power variations: (a) Output power from wind conversion system (b)

Load power demand (c) Power absorbed and released by battery (d) Power dealt by SMES.

Fig. 10 gives the power variations. It is obvious that the power output from the wind turbine contains a large amount of high frequency component as shown in Fig.10 (a). As can be seen Fig.10 (a) and (b), the generated power cannot always match the load requirement. Hence, the battery and SMES come to work to deal with the surplus or the deficient power. As the HESS has been designed, the battery is charged and discharged by the low-frequency component while SEMS offers short term high-frequency support to the power difference, as illustrated in Fig. 10(c) and (d). Also, two hours variation are shown in small window in Fig. 10(c) and (d). It can be seen that SMES has dramatically fast response to the high-frequency demand while battery is responsible for the low-frequency demand.

The comparisons of battery in two conditions (battery only ESS and HESS) are shown in Fig. 11 with low-pass filter cut-off frequency of 0.002 Hz. In terms of battery current, mainly two differences can be observed from Fig. 11: compared with battery only ESS, battery current in HESS undergoes significantly fewer polarity reversals and the peak value is relatively smaller than that in battery only ESS. Consequently, the battery in HESS experienced not only quite fewer charge/discharge cycles but also lower DODs as can be seen out in Fig. 11.

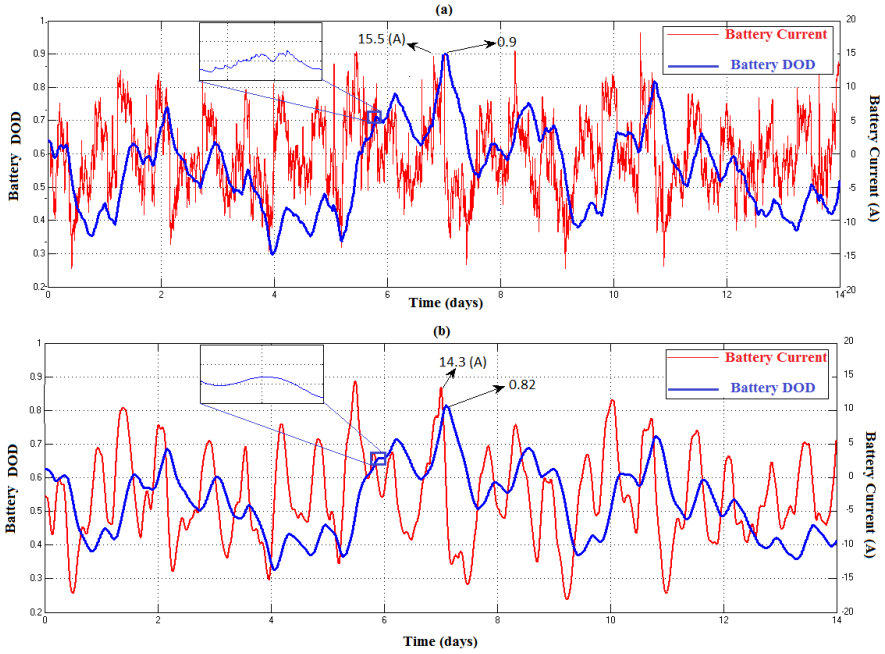

Fig. 11. Simulation results of battery current and DOD: (a) Battery only ESS (b) Battery and SMES HESS (Blue line represents the DOD of battery and red line gives the charge/discharge current)

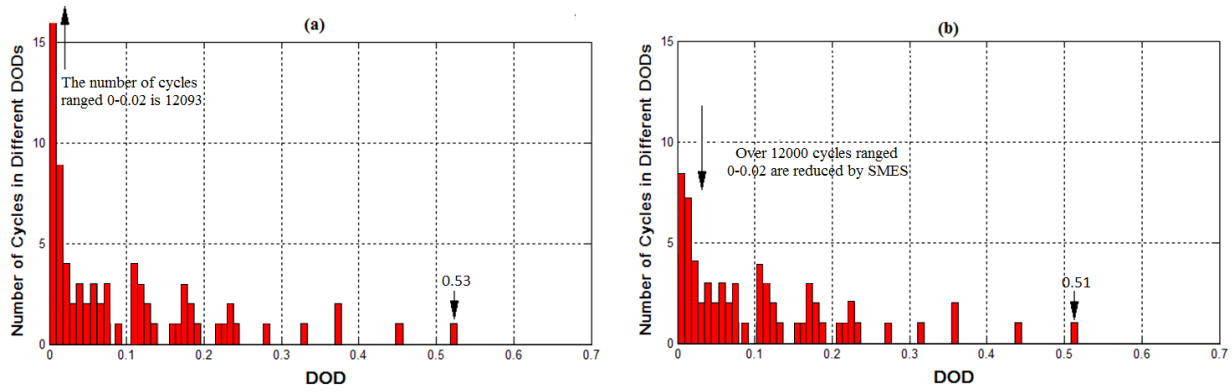

Fig. 12. Histograms of Number of Cycles in Different DODs: (a) Battery Only ESS, (b) SMES-battery HESS

Histograms to describe the number of battery cycles at different DODs in each system can be obtained by running the improved rain-flow counting algorithm and are shown in Fig.12.

As it can be observed from Fig.12 the battery in the HESS experienced extensively fewer small cycles which are characterized by short-range (<0.02) DODs. Also, the depth of each cycle is reduced especially for the large cycles. For example, the DOD of the deepest cycle in battery only energy storage system is 0.53 whereas for the SMES-battery HESS is 0.51. This highlights that not only small charge/discharge cycles of battery but also the peak value of battery discharging can be reduced by using SMES. Furthermore, this paper defines the battery life degradation factor η (Eq. (12)) to described to what extent the cycle depredated the battery for a given DOD and Crate. The bigger the factor is, the more damage the battery would undergo. Fig. 13 gives the 3-D plots of all the cycles with different DODs, Crates and degradation factors experienced by batteries in the two systems during the simulation period.

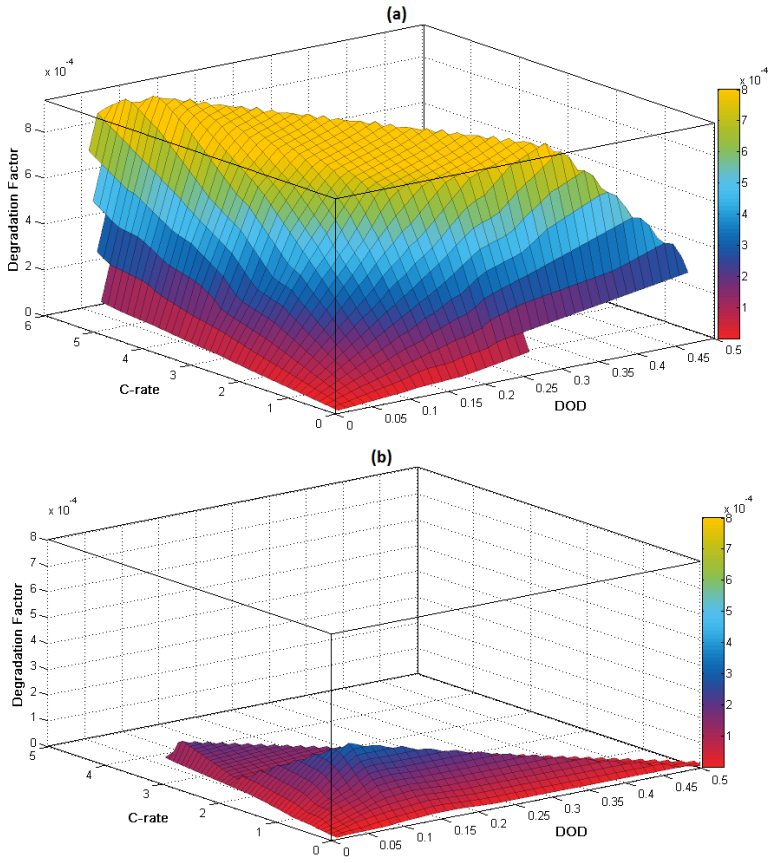

Fig. 13. 3-D plot describe the degradation factor effected by both DOD and Crate: (a) Battery only ESS, (b) SMES-battery HESS

Fig. 13 gives a visualized tendency of less damage to battery in a HESS. As shown in Fig. 13, the HESS highlights two features compared with the battery only ESS: Firstly, the much narrower region of Y- axis (Crate) means the lower Crate or discharging current; Secondly, the smaller area of the plotted figure and lower value of degradation factors proves the synergic impact of the reduced cycle numbers and the decreased discharging current.

The battery lifetime for each system is determined by the novel battery life-cycle model. In case of battery only ESS, the batteries can be used for 8.7 years whereas for the HESS, the battery lifetime can reach as high as 11.5 years achieving 32.18% increase. A larger time constant of low-pass filter means a lower cut off frequency which results in more extension of battery lifetime. However, a bigger size of SMES results in higher investment and larger power losses. In this paper, the 32.18% improvement of battery lifetime can be achieved by a 2 kJ SMES.

The simulation results and followed analysis above has successfully proved the benefits of the designed SMES-battery HESS. The fluctuation and intermittency of wind power is compensated by the HESS and the load demand is met. Based on the proposed system and the novel battery life-time model, battery lifetime in the SMES-battery hybrid system is quantifiably increased, which is quite meaningful for the applications where battery is expected to be replaced multiple times. It should be figured out that the SMES systems are costly because of the expensive superconductive material cost and this is a disadvantage of the proposed HESS. However, with the continuous developing of

superconductive materials science many published researches [46-49] have shown positive cost-effective analysis of SMES. For the future prospect of SMES and battery HESS, the Strengths, Weaknesses, Opportunities and Threats (SWOT) analysis is presented in Table [12, 18, 48-50].

Table 4 SWOT analysis of SMES and battery HESS

Positive	**Negative**
Strengths • High response speed (within milliseconds) • Large power density enabled by SMES • Large energy density enabled by battery • High efficiency • Infinite charge and discharge cycles (SMES)	Weaknesses • Expensive material cost at the present stage • Need cooling system • Need complicated control to achieve an active integration of SMES and battery • Instability of superconductors in the loss of cooling power
Opportunities • Battery lifetime extension • Lower rated energy equipment of SMES resulting in investment reduction • Decreasing material cost due to developing materials science • Large power density enable oscillation damping, power factor correction • Large energy density enable energy management function	Threats • Quench problems of SMES coil • Limited existing examples and experiences of the SMES and battery HESS • Impact on the traditional electric device • Instability of the power electronic devices used for control • Health risk caused by the stray magnetic field

5 Conclusion

This study has investigated the use of a SMES-battery hybrid energy storage system in a small scale off-grid wind power system. A representative dynamic off-grid power system with HESS is established in Matlab/Simulink. SMES and batteries are successfully hybridized achieving a stable and fast-responded HESS to mitigate the fluctuations of wind power and balance the power supply and load demand. A novel battery life-cycle model which has considered both the depth of discharge and discharging rate of battery is proposed and gave a more accurate prediction. The lifetime of battery is improved in the HESS by reducing the charge/discharge frequency and lowering high discharging rate and the extension of battery life is quantified by using the novel battery life-cycle model. Future detailed economic cost-benefit analysis of an optimal matching of HESS with renewable power can be achieved based on the novel battery lifetime model. In addition, the proposed battery lifetime model can be potentially used in other applications.

Acknowledgements

All the Authors would like thanks the support by EPSRC EP/K01496X/1, Royal Academy of Engineering, UK and the State Key Lab of Power System in Tsinghua University, China. Jianwei Li would like to thanks the support by Chinese Scholarship Council, China.

Appendix

Table A1 Wind-turbine model parameters

Cut-in Wind Speed	2.5 m/s
Cut-Out Wind Speed	None
Rated Power	1000 watts
Rated Wind Speed	11 m/s
Rotor Diameter:	2.5 m
Rotor moment of inertia	2.0 kg/m2
Generator moment of inertia	1.0kg/ms2
Damping coefficient	0.00035 Nm/rad/s

Table A.2 The Designed 2kJ SMES parameters

Conductor Length	≈600m
Number of coils	5
Maximum magnetic flux density	≈2.5T
Total Height	50mm
Inductance	≈ 0.7 H
Operation current	80A

Reference

[1] Díaz-González F, Sumper A, Gomis-Bellmunt O, Villafáfila-Robles R. A review of energy storage technologies for wind power applications. Renewable and Sustainable Energy Reviews. 2012;16(4):2154-71.

[2] Krieger EM, Cannarella J, Arnold CB. A comparison of lead-acid and lithium-based battery behavior and capacity fade in off-grid renewable charging applications. Energy. 2013;60(0):492-500.

[3] Svoboda V, Wenzl H, Kaiser R, Jossen A, Baring-Gould I, Manwell J, et al. Operating conditions of batteries in off-grid renewable energy systems. Solar Energy. 2007;81(11):1409-25.

[4] Bhattacharyya SC. Review of alternative methodologies for analysing off-grid electricity supply. Renewable and Sustainable Energy Reviews. 2012;16(1):677-94.

[5] Thackeray MM, Wolverton C, Isaacs ED. Electrical energy storage for transportation—approaching the limits of, and going beyond, lithium-ion batteries. Energy & Environmental Science. 2012;5(7):7854-63.

[6] Li N, Chen Z, Ren W, Li F, Cheng H-M. Flexible graphene-based lithium ion batteries with ultrafast charge and discharge rates. Proceedings of the National Academy of Sciences. 2012;109(43):17360-5.

[7] Ferreira HL, Garde R, Fulli G, Kling W, Lopes JP. Characterisation of electrical energy storage technologies. Energy. 2013;53(0):288-98.

[8] Kim YM, Shin DG, Favrat D. Operating characteristics of constant-pressure compressed air energy storage (CAES) system combined with pumped hydro storage based on energy and exergy analysis. Energy. 2011;36(10):6220-33.

[9] Boukettaya G, Krichen L, Ouali A. A comparative study of three different sensorless vector control strategies for a Flywheel Energy Storage System. Energy. 2010;35(1):132-9.

[10] Zhao P, Dai Y, Wang J. Design and thermodynamic analysis of a hybrid energy storage system based on A-CAES (adiabatic compressed air energy storage) and FESS (flywheel energy storage system) for wind power application. Energy. 2014;70(0):674-84.

[11] Mellincovsky M, Kuperman A, Lerman C, Aharon I, Reichbach N, Geula G, et al. Performance assessment of a power loaded supercapacitor based on manufacturer data. Energy Conversion and Management. 2013;76(0):137-44.

[12] Zhu J, Qiu M, Wei B, Zhang H, Lai X, Yuan W. Design, dynamic simulation and construction of a hybrid HTS SMES (high-temperature superconducting magnetic energy storage systems) for Chinese power grid. Energy. 2013;51(0):184-92.

[13] Barton JP, Infield DG. Energy storage and its use with intermittent renewable energy. IEEE Transactions on Energy Conversion, . 2004;19(2):441-8.

[14] Khaligh A, Li Z. Battery, ultracapacitor, fuel cell, and hybrid energy storage systems for electric, hybrid electric, fuel cell, and plug-in hybrid electric vehicles: State of the art. IEEE Transactions on Vehicular Technology. 2010;59(6):2806-14.

[15] Moreno J, Ortúzar ME, Dixon L. Energy-management system for a hybrid electric vehicle, using ultracapacitors and neural networks. IEEE Transactions on Industrial Electronics. 2006;53(2):614-23.

[16] Li W, Joós G, Bélanger J. Real-time simulation of a wind turbine generator coupled with a battery supercapacitor energy storage system. IEEE Transactions on Industrial Electronics. 2010;57(4):1137-45.

[17] Sarrias-Mena R, Fernández-Ramírez LM, García-Vázquez CA, Jurado F. Fuzzy logic based power management strategy of a multi-MW doubly-fed induction generator wind turbine with battery and ultracapacitor. Energy. 2014;70(0):561-76.

[18] Ise T, Kita M, Taguchi A. A hybrid energy storage with a SMES and secondary battery. Ieee T Appl Supercon. 2005;15(2):1915-8.

[19] Zhou H, Bhattacharya T, Tran D, Siew TST, Khambadkone AM. Composite energy storage system involving battery and ultracapacitor with dynamic energy management in microgrid applications. IEEE Transactions on Power Electronics. 2011;26(3):923-30.

[20] Gee AM, Robinson FVP, Dunn RW. Analysis of Battery Lifetime Extension in a Small-Scale Wind-Energy System Using Supercapacitors. IEEE Transactions on Energy Conversion. 2013;28(1):24-33.

[21] Manwell JF, McGowan JG, Abdulwahid U, Wu K. Improvements to the Hybrid2 battery model. American Wind Energ Association Windpower 2005 Conference. American Wind Energy Association. Colorado. 2005.
[22] Guan T, Zuo P, Sun S, Du C, Zhang L, Cui Y, et al. Degradation mechanism of LiCoO2/mesocarbon microbeads battery based on accelerated aging tests. Journal of Power Sources. 2014;268(0):816-23.
[23] Dufo-López R, Bernal-Agustín JL, Yusta-Loyo JM, Domínguez-Navarro JA, Ramírez-Rosado IJ, Lujano J, et al. Multi-objective optimization minimizing cost and life cycle emissions of stand-alone PV–wind–diesel systems with batteries storage. Applied Energy. 2011;88(11):4033-41.
[24] Vichare N, Rodgers P, Eveloy V, Pecht MG. In situ temperature measurement of a notebook computer-A case study in health and usage monitoring of electronics. IEEE Transactions on Device and Materials Reliability. 2004;4(4):658-63.
[25] Das DC, Roy A, Sinha N. GA based frequency controller for solar thermal–diesel–wind hybrid energy generation/energy storage system. International Journal of Electrical Power & Energy Systems. 2012;43(1):262-79.
[26] Vlad C, Munteanu I, Bratcu AI, Ceangă E. Output power maximization of low-power wind energy conversion systems revisited: Possible control solutions. Energy Conversion and Management. 2010;51(2):305-10.
[27] Sawetsakulanond B, Kinnares V. Design, analysis, and construction of a small scale self-excited induction generator for a wind energy application. Energy. 2010;35(12):4975-85.
[28] Nie ZX, Xiao X, Kang Q, Aggarwal R, Zhang HM, Yuan WJ. SMES-Battery Energy Storage System for Conditioning Outputs From Direct Drive Linear Wave Energy Converters. Ieee T Appl Supercon. 2013;23(3):5000705-.
[29] Bakelli Y, Hadj Arab A, Azoui B. Optimal sizing of photovoltaic pumping system with water tank storage using LPSP concept. Solar Energy. 2011;85(2):288-94.
[30] Ould Bilal B, Sambou V, Ndiaye P, Kébé C, Ndongo M. Optimal design of a hybrid solar–wind-battery system using the minimization of the annualized cost system and the minimization of the loss of power supply probability (LPSP). Renewable Energy. 2010;35(10):2388-90.
[31] Zhou W, Lou C, Li Z, Lu L, Yang H. Current status of research on optimum sizing of stand-alone hybrid solar–wind power generation systems. Applied Energy. 2010;87(2):380-9.
[32] Tixador P. Superconducting magnetic energy storage (SMES) systems. In: Melhem Z, editor. High Temperature Superconductors (HTS) for Energy Applications: Woodhead Publishing; 2012. p. 294-319.
[33] Yuan W, Xian W, Ainslie M, Hong Z, Yan Y, Pei R, et al. Design and test of a superconducting magnetic energy storage (SMES) coil. IEEE Transactions on Applied Superconductivity,. 2010;20(3):1379-82.
[34] Gu W, Sun Z, Wei X, Dai H. A New Method of Accelerated Life Testing Based on the Grey System Theory for a Model-Based Lithium-Ion Battery Life Evaluation System. Journal of Power Sources. 2014.
[35] Dufo-López R, Bernal-Agustín JL, Domínguez-Navarro JA. Generation management using batteries in wind farms: Economical and technical analysis for Spain. Energy policy. 2009;37(1):126-39.
[36] Bindner H, Cronin T, Lundsager P, Manwell JF, Abdulwahid U, Baring-Gould I. Lifetime modelling of lead acid batteries. Risø Nat.Lab. Roskilde, Denmark; 2005.
[37] Garcia B, Lavallée S, Perron G, Michot C, Armand M. Room temperature molten salts as lithium battery electrolyte. Electrochimica Acta. 2004;49(26):4583-8.
[38] Ecker M, Gerschler JB, Vogel J, Käbitz S, Hust F, Dechent P, et al. Development of a lifetime prediction model for lithium-ion batteries based on extended accelerated aging test data. Journal of Power Sources. 2012;215:248-57.
[39] Van Bree B, Verbong GP, Kramer GJ. A multi-level perspective on the introduction of hydrogen and battery-electric vehicles. Technological Forecasting and Social Change. 2010;77(4):529-40.
[40] Ning G, Haran B, Popov BN. Capacity fade study of lithium-ion batteries cycled at high discharge rates. Journal of Power Sources. 2003;117(1):160-9.
[41] Niesłony A. Determination of fragments of multiaxial service loading strongly influencing the fatigue of machine components. Mechanical Systems and Signal Processing. 2009;23(8):2712-21.

[42] Jeong D, Lee J. Electrode design optimization of lithium secondary batteries to enhance adhesion and deformation capabilities. Energy. 2014;75(0):525-33.
[43] Wang D, Li H, Shi S, Huang X, Chen L. Improving the rate performance of LiFePO4 by Fe-site doping. Electrochimica Acta. 2005;50(14):2955-8.
[44] Omar N, Bossche PVd, Coosemans T, Mierlo JV. Peukert Revisited—Critical Appraisal and Need for Modification for Lithium-Ion Batteries. Energies. 2013;6(11):5625-41.
[45] Zhang Q, White RE. Capacity fade analysis of a lithium ion cell. Journal of Power Sources. 2008;179(2):793-8.
[46] Malozemoff A, Fleshler S, Rupich M, Thieme C, Li X, Zhang W, et al. Progress in high temperature superconductor coated conductors and their applications. Superconductor Science and Technology. 2008;21(3):034005.
[47] Yamada Y, Hattori T. Development of cost-effective HTS superconductor.: Simple heat treatment and low-cost substrate Ni/NiO. Physica C: Superconductivity. 2000;335(1):78-82.
[48] Nomura S, Watanabe N, Suzuki C, Ajikawa H, Uyama M, Kajita S, et al. Advanced configuration of superconducting magnetic energy storage. Energy. 2005;30(11–12):2115-27.
[49] Suzuki S, Baba J, Shutoh K, Masada E. Effective application of superconducting magnetic energy storage (SMES) to load leveling for high speed transportation system. Ieee T Appl Supercon. 2004;14(2):713-6.
[50] Chen H, Cong TN, Yang W, Tan C, Li Y, Ding Y. Progress in electrical energy storage system: A critical review. Progress in Natural Science. 2009;19(3):291-312.